Analysis Between the Rothermel and Balbi Fire Spread Model

By: Jeremy Benik, Adam Kochanski, John Stuart, Aurelien Costes

February 7, 2023

1 Abstract

Accurately predicting the rate of spread (ROS) of a propagating fire in various fuels, weather, and topography poses as quite the challenge given the complexities of fire. Such as the small-scale processes occurring that must be taken into consideration to produce an accurate calculation for the ROS. To predict the ROS, multiple models have been created to predict the ROS in varying environments and atmospheric conditions. These models prove invaluable to those who model wildfires as they allow modelers to run simulations and generate forecasts for wildfires. A comparison of different ROS models will allow for the most accurate model to be determined and implemented to improve future forecasts and simulations. The two fire ROS models in this study are the Rothermel model and the Balbi model. These two models aim to accurately predict fire spread in various conditions, however, the way they calculate the ROS differs from one another. The Rothermel model is a semi-empirical model that was created in 1972, and the Balbi model is a physics-based model that is still being worked on to this day (with the most recent model being released in 2022). Within these models, varying assumptions are made about how each mechanism within a fire contributes to the overall ROS. Conceptually, the models also differ since the Rothermel model is a semi-empirical model and the Balbi model is a fully physical model. To see how each model performs, the models were converted into a MATLAB code and various tests were performed on each model. These tests include changing parameters within the fuels, topography, fuel moisture, and weather conditions to see how each factor influences the models. Smaller scale processes within the code that lead up to the overall ROS were analyzed to evaluate how each calculation within the code weighs into the final calculations.

To see which model performs best in an operational setting, the models were compared using the 13 Albini fuels. This dataset is currently implemented across an array of models (such as WRF-SFIRE and BEHAVE) as it covers a wide variety of different fuel types. Using this dataset, the ROS between each model can be accurately compared since they will be tested under the same fuel type and conditions.

2 Introduction

Providing an accurate assessment of the rate of spread (ROS) of a fire in varying environmental conditions and topography poses as a challenging task. Many small-scale processes occur both within a fire (such as the amount of heat released from the fire) and interactions between the fire and weather/terrain. Formulating an accurate model that can predict the ROS in varying fuels and weather conditions would serve as an invaluable resource for fire modelers. It can also be implemented into other fire models to provide an accurate prediction of where a fire may spread. With this knowledge, fire managers can use different tactics to control and extinguish fires much faster than before. There are three types of models that predict the ROS, 1. empirical models, 2. semi-empirical models, 3. physical models. Empirical models use statistical data and observational data to figure out the ROS. These models lack any physical characteristics and are usually simplified models. Semi-empirical models use both observational data and physical properties to calculate the rate of spread. Models like these have proven to be useful with calculating the ROS as these models simplify fire spread processes while incorporating key principles [Chatelon et al., 2022]. Physical models are solely based on physical and chemical processes occurring within a fire. For physical models, they are based on a series of complex partial differential equations and include principles from fluid dynamics that can make solving the equations necessary for the ROS computationally challenging and time consuming. By simplifying these principles and making a few assumptions, some models are able to still provide an accurate calculation of the ROS in less compute time.

Larger scale models that predict where the fire will spread (such as WRF-SFIRE) utilize ROS models to determine how fast the fire will spread in a certain environment. 2 ROS models that are currently in use across an array of the larger scale models are the Balbi model and the Rothermel model. The Balbi model is a physics-based model which aims to provide computationally fast and accurate simulations of fire propagation with the idea that fire managers can use them under operational conditions [Chatelon et al., 2022]. The Balbi model has undergone many revisions over the past 15 years and is still being worked on to this day. The Rothermel model is a semi-empirical model that was created by Richard C. Rothermel in 1972 and has undergone revisions by Frank A. Albini in 1976 [Anderson et al., 2010]. The goal of this model is to accurately calculate fire spread in different environments with only a few inputs necessary.

2.0.1 Rothermel Model

The Rothermel model is based on a heat balance model developed by Fransden (1971) and it incorporates data obtained from wind tunnel experiments in artificial fuel beds containing various fuels, and from Australian wildfire data in grasses [Anderson et al., 2010]. From these datasets, Rothermel was able to use observational data along with physical properties to create the model. This model still contains a lot of assumptions and is nowhere near perfect. There are still limitations with this model, but it can still provide a decently accurate ROS calculation in a timely manner.

The formulation of this model is still quite complex despite it not being a fully physical model and making assumptions about some properties. In the beginning, the ROS equation was solely based on the conservation of energy equations which made the initial equation difficult to solve. By using observations and an understanding of how fire propagates in certain environments, simplifications were made to the model that made the calculations much more simple. As a result, the model can be solved not only by humans, but codes of the model can be created and solved almost instantaneously by a computer.

To reduce the initial complex equation to the final form (as seen in equation 22), small details were implemented into the model to reduce the complexity, but retain the accuracy. For a fire to spread, the fire must preheat the potential fuels to ignition temperature. To ignite the fuel, it depends on ignition temperature, moisture content, and the amount of fuel involved [Rothermel, 1972]. The way a fire can preheat the fuels varies too. Certain components within a fire can preheat the fuels more than other components in different scenarios. An example of this is the horizontal propagating flux and the vertical propagating flux. In a no wind situation, the horizontal propagating flux would dominate fire spread, but when wind or a slope is introduced, the vertical propagating heat flux dominates since there is more direct flame contact and convective heat transfer to the fuels.

The next component in Rothermel's paper is the reaction intensity (I_R). This is the energy released by the fire front and is produced by burning gases released from the organic matter in the fuels [Rothermel, 1972]. The reaction intensity is mainly based on the fuel type but knowing the intensity aids in developing the model. This also changes with wind and slope as the propagating heat flux exposes the fuel to additional convective and radiant heat transfer. With just this knowledge so far, Rothermel was able to simplify the main equation down to a handful of variables without any need of calculus.

To finish up the model, Rothermel ran a series of experiments to gather the last few missing parameters (such as the reaction velocity, mineral damping coefficient, and moisture damping coefficient). To find these parameters, he constructed weighing platforms to support the fuel for the fuel beds and supported the beds with four load cells which had ceramic cylinders and baffles to protect it from the heat [Rothermel, 1972]. All the load cells contained electronics that would take measurements during the burn. With this experiment, Rothermel was able to implement the missing parameters into his model without accounting for wind or slope impacts. Similar experiments were conducted to find how the slope and wind impacts the ROS. To find the wind coefficient, Rothermel used McArthurs dataset on the grassland fires in Australia and a wind tunnel in a laboratory. After these experiments, Rothermel came up with a correlation between the wind speed and the ROS as a function of the fuel type and fuel load. As for the slope coefficient, he used fuel beds and sloped the beds at 25, 50, and 75 percent and had varying packing ratios [Rothermel, 1972]. After this experiment he came up with a correlation for the slope parameter.

After all these experiments, the complete set of parametric equations were finally developed [Rothermel, 1972], but the model still is not yet suitable for field use since it was created in lab setting. With different compositions of fuels in the environment, the model cannot properly account for these and accurately calculate the ROS. To combat this, Rothermel created the concept of a fuel cell which is the smallest column of fuel within a stratum of mean depth that has sufficient fuel to be statistically representative of the fuel in the entire fuel complex [Rothermel, 1972]. The fuel cell concept is used to weigh the input parameters and not

to have specific values provided for the fuels. Instead, mean values that quantify the modeled fuel complex. By adding in these mean values and modifying the model, it can be used at a field scale. While this model still has limitations, for its time it was easily the best model out there.

Once the initial model was complete, Rothermel began working on developing the wind and slope coefficients. The wind coefficient was calculated by building multiple fuel beds in a wind tunnel and running the wind tunnel at 2, 4, 6, or 8 mph and calculating the ROS as well as comparing the model to McArthur's dataset. With these data, Rothermel was able to develop a correlation between the wind speed and ROS. He also found that certain fuel properties affect the wind coefficient so he implemented those fuel properties into the wind coefficient. The slope coefficient was created a similar way. Multiple fuel beds were constructed at different slopes and Rothermel found a relationship between the slope of the fuel beds and the ROS. He also incorporated the packing ratio into the coefficient since that affects the ROS on sloped terrain.

2.0.2 Balbi Model

The Balbi model is a physical model developed by Jacques-Henri Balbi, Jean-Louis Rossi, Thierry Marcelli, and Paul-Antoine Santoni [Balbi et al., 2007]. The Balbi model is proposed as a model that can run faster than real time and will be integrated into management tools [Balbi et al., 2007]. The goal of this model is to be as complete as possible with regards to the equations that govern fires and be as simple as possible to predict fire spread faster than real time [Balbi et al., 2007]. Since this model is fully physics based, many simplifying assumptions are necessary to get the model to a point where it can be used at an operational point since the main equations governing fire spread would take too long to compute for operational use.

In the Balbi model, a major part of the overall calculation time comes from the equations governing the flow [Balbi et al., 2007]. To combat this issue, major simplifications are made to the model to simplify it as much as possible while still retaining an accurate and fast result. An example occurs in the calculation of the free stream wind and upward gas flow velocity in still air [Balbi et al., 2007]. To calculate these parameters, multiple physical processes such as thermal balance and radiant heat flux must be considered. To reduce this down to simple calculations, the authors split up a flame into two different properties, the flame base and the embers, and the flame body. By adding these two components, that should yield the resulting radiant heat flux and thermal balance. For the flame base radiation, this component deals more with distance from the unburnt fuel to the flame base and emissivity of the fire. As for the flame body, this component takes over with a slope or windy conditions since the flames are brought closer to the unburnt fuel, resulting in more radiative heat flux impinging on the fuel [Balbi et al., 2007].

Like with Rothermel, accounting for slope and wind speed in the model added another layer of complexity to the model. Equations were first developed with the simplifying assumption of no slope and no winds, then later slope and wind would be added into the model. Their equations incorporating slope and wind ended up producing a series of nonlinear equations, which would increase the computational time of the model. As a result, they used algorithms in Mathematica to find a solution for these equations. There were still some parameters missing within the model that could only be found with testing, but for now the model could be tested and compared to real simulation.

For testing the model, Balbi used 3 different sets of laboratory experimental data. The first test occurred with both slope and windy conditions in Lisboa, Portugal. The results of this first experiment proved promising as there was a relative error of 6.54% with a correlation coefficient of 0.9836 [Balbi et al., 2007]. Some adjustments to the model had to be made, but these changes improved on the model and added some more constants to make calculations easier in the future. The next experiment was conducted in the combustion tunnel of INIA [Balbi et al., 2007]. The main goal of this experiment was to test the model with varying winds. Winds ranged from 1 to 3m/s. There were also 2 different fuel load values, and three replications per wind speed and fuel load. With this experiment, Balbi found some of the fitted parameters from the last experiment did not fit in this experiment, and there were deviations between the two experiments. Some parameters remained relatively constant throughout the experiments and those parameters became constant in the model. The last experiment occurred at the University of Combra under wind or upslope conditions [Balbi et al., 2007]. The wind speeds varied between 1.5 to 4.5m/s and the fuel bed was set anywhere from 0 to 40 degrees. By testing the model in both no wind with slope, and wind with no slope conditions, the model fit parameters could be tested again. With the slope and wind parameters they calculated from previous experiments, they were input into the model, and the model performed well. No statistics were given in this study, instead there were plots of the observed ROS compared to the modeled ROS. One important note is the slope factor and the wind factors are different (as predicted in the model), and these parameters fit high slope and high winds which other literature underestimates [Balbi et al., 2007]. As a result of these

experiments, the model has been fit for laboratory experiments.

To get the model fit for field scales, an analysis of 29 field-scale experiments were performed for varying vegetation and winds. There was no slope in these experiments. With a statistical study, Martins Fernandes (author of the paper) derived a model that fits the parameters that were causing problems in the laboratory experiments [Balbi et al., 2007]. Except this time these are for field-scales. With this analysis, the model is now claimed to be able to be used at a field scale and laboratory scale with some of the same parameters as before, and with the changing parameters being dependent on the vegetation. Overall, this model satisfies what the authors were originally looking for. It is a faster than real time model that is fully physical. This is just the beginning of the model as there have been many changes throughout the years that have led to this model getting more accurate.

With more research into how fires spread, the Balbi model has evolved quite a bit. One question remains unanswered in the Balbi model that needs to be addressed and that is what the dominant heat transfer mode is [Balbi et al., 2020]. Some models began removing certain parameters since they did not think they contributed to the ROS. In this model, the authors take a closer look at how convective heat transfer impacts the ROS. To test a convective heat transfer component, they used multiple laboratory experiments. By running these experiments in a laboratory setting, the authors were able to better determine what processes are the leading cause of the ROS along with finding finer details about each process that contribute to the ROS. Two terms that are new in the model are convective cooling and the flame base radiation. With the addition of these two parameters, it adds more complexity to the model, but overall, it accounts for more processes within a fire which could provide a more accurate ROS.

After extensive testing and modifying the model with their lab setting and more than 300 experimental fires, the model was found to have an error below 8% compared to the observed ROS which proves as a satisfactory result for the authors [Balbi et al., 2020]. This model is still claimed to faster than real time and it can be used at much larger scales. The model also has no parameter that varies between experiments, which makes this model fully predictive [Chatelon et al., 2022].

The last modifications (and most current as of writing) occurred this year in 2022. This year, the Balbi model was modified further to better account for field scale fires. Before, the model was built off laboratory experiments which still proved useful as the results from the 2020 paper show, but now the model can be better applied in the field. Some notable changes between the two models include removing certain parameters to account for field scales and setting some values constant. This model also better considers convective and radiative heat transfer as heat transfer mechanisms and can be used under operational conditions [Chatelon et al., 2022]. One parameter of interest in this study was the fitted model parameter. The goal of this was to provide a coefficient that would allow this model to be used at an operational setting. After running the model on various field experiments the authors were able to come up with a parameter that better calculates the ROS. Sensitivity analyses were also done on this model to see what parameters contributed most to the ROS. The authors found that convection was the main heat transfer mechanism driving fire propagation [Chatelon et al., 2022].

With the introduction of a convective component, there have been further studies to determine the fine scale processes going on in convective heat transfer. Anderson et al., 2010, performed multiple experiments to test how heat transfer through convection occurs. These tests were done in a wind tunnel at the USDA Forest Service Sciences Laboratory in Missoula, Montana [Anderson et al., 2010]. In these experiments, Anderson laid out various fuels and instrumentation within the burn plot to characterize the gas temperature (air and pyrolysates) and the flow that drives convective heating of unburnt fuels ahead of the fire [Anderson et al., 2010]. By running the experiments in both windy and no-wind conditions, they could determine how much wind affects convective heat transfer. They found that the gas temperature was greater with minimal wind. As the wind speeds increased above 1m/s there was an exponential maximum gas temperature. A decrease in the gas temperature was also noted with an increased fuel packing ratio and moisture content. Next is the surface gas velocity. In this experiment, they laid out fuel in a way that some fuel elements were farther away from each other. The fuels that were considered far away from other fuels (about 1.8m) did not show much change in the surface velocity under constant wind speed. With an increase in wind speed however, the surface velocity increased as well. For fuels in the middle region (0.3-1/7m), there was a rapid decrease in the surface wind [Anderson et al., 2010]. In fact, this would lead to a reversal in the flow approaching the flame front [Anderson et al., 2010]. With tightly packed fuels, there was a rapid increase in the surface wind from the minimum value to the maximum value.

By comparing the two models using different fuels and weather conditions, each component within the model can be evaluated to see what contributes the most to the ROS. With this knowledge, certain compo-

nents within a fire (such as fire-induced circulations) can be better evaluated and calculated in future models to better calculate the ROS. With a more accurate ROS model, this will improve bigger fire models. With a more accurate model, that can help fire managers better decide where the fire will spread and how fast it will spread to a certain area. Improvements in the models will also aid in our understanding of fine scale processes occurring within a fire. These improvements will likely be with modern models (such as the Balbi model) and not older models, but overall, any improvements could help fire managers better control fire spread.

3 Methods

To compare the two rates of spread models both conceptually and analytically, papers from both models as well as MATLAB codes from both models were used to better understand the underlying equations, constants, and assumptions behind each model. By comparing the papers to the MATLAB code and evaluating how each parameter fits in the overall ROS, it was much easier to understand how much each parameter contributes to the ROS.

To analyze the models analytically, the two MATLAB functions (link to them is in Appendix A) were modified to accept more input parameters as well as accept multiple values as an input. Before the modification, the codes could only accept the fuel type, wind speed, slope, and fuel moisture. After the modification the codes could accept another input parameter (named input in the code), that can be assigned to any value. Originally the code cannot accept an array, but with modifying the equations to accept an array and output the ROS components as an array, the results can then be plotted and evaluated to determine how that parameter impacts the overall ROS. The last change occurred in the Rothermel function. Originally, the model caps the ROS at 6m/s however for this analysis this was removed to observe how the model behaves under extreme conditions. Lastly, the fuel of choice for testing the models is tall grass (2.5ft) since is is a grass type fuel and small changes to it will make a noticeable impact to the ROS.

4 Results

4.1 Rothermel Model

4.1.1 Initial Rate of Spread Equation

The initial Rothermel model was based on the heat balance model developed by Fransden (1971) and can be see in equation 1.

$$R = \frac{I_{xig} + \int_{-\infty}^{0} (\frac{\partial I_z}{\partial z})_{z_c} \, dx}{\rho_{be} * Q_{i_g}} \tag{1}$$

Where R = Quasi-steady rate of spread, ft./min.

I_{xig} = Horizontal heat flux absorbed by a unit volume of fuel at the time of ignition, $B.t.u/ft.^2$ -min

ρ_{be} = Effective bulk density (the amount of fuel per unit volume of the fuel bed raised to ignition ahead of the advancing fire), lb./ft.3

Q_{ig} = Heat of preignition (the heat required to bring a unit weight of fuel to ignition),. B.T.U./lb

$(\frac{\partial I_z}{\partial z})_{z_c}$ = The gradient of the vertical intensity evaluated at a plane at a constant depth, z_c, of the fuel bed, B.t.u./ft.^{3} -min

With equation 1 being the starting equation, there was a lot of work necessary to reduce it down to the final equation. Especially when slope and wind is considered, then formulating the model becomes much more complex. To help reduce the complexity, the initial ROS equation was formulated assuming no slope and no wind conditions.

The next step within the model is to evaluate each parameter within equation 1 and simplify it to make the final equation able to be quickly solved without reducing accuracy.

4.1.2 Heat of Preignition (Q_{ig})

The first equation evaluated was the heat of preignition Q_{ig}. This term was "evaluated analytically for cellulosic fuels by considering the change in specific heat from ambient to ignition temperature and the latent heat of vaporization of the moisture" [Rothermel, 1972]. This resulted in equation 2.

$$Q_{ig} = C_{pd}\Delta T + M_f(C_{pw}\Delta T_B + V) \tag{2}$$

Where:
C_{pd} = Specific heat of dry wood.
ΔT_{ig} = Temperature range to ignition
M_f = Fuel moisture. lb. water/lb. dry wood.
C_{pw} = Specific heat of water.
ΔT_B = Temperature range to boiling.
V = Latent heat of vaporization.

To further reduce this equation down to the final form, an assumption was made that the temperature to ignition will stay at a constant range from 20°C to 320°C and that boiling temperature will remain at 100°C, and that the fuel will remain a cellulosic fuel, the equation then became:

$$Q_{ig} = 250 + 1116 * M_f.B.T.U/lb. \tag{3}$$

These assumptions take out the need for the temperature range to ignition, latent heat of vaporization, temperature range to boiling, and specific heat of dry wood. With less parameters necessary, the model becomes much more simple and faster (computationally). This also aids in reaching Rothermel's goal of creating a ROS model with as few input parameters as possible.

4.1.3 Effective Bulk Density (ε)

The next parameter is the effective bulk density (ε) . This parameter was calculated experimentally using thermocouples laid out in a fuel bed. The effective bulk density is used in the final rate of spread equation with no wind and no slope (r0). The equation for effective bulk density can be seen in equation 4.

$$\varepsilon = \exp(-138/\sigma) \tag{4}$$

Where:
σ = Surface Area to Volume Ratio. ft $^{-1}$

4.1.4 Reaction Intensity (I_R)

The next parameter is the reaction intensity. This is by far the hardest to calculate as it is the most complex to derive. To obtain this value, the authors used the weight loss data from the fuels to determine how intense the fire was. This parameter can be expressed as equation 5.

$$I_R = -(\frac{\mathrm{d}w}{\mathrm{d}x})(\frac{\mathrm{d}x}{\mathrm{d}t})h \tag{5}$$

Where :
$\frac{\mathrm{d}x}{\mathrm{d}t}$ = R, the quasi steady state rate of spread.

By integrating the equation with respect to the reaction zone depth D, that results in equation 6.

$$I_R D = Rh(W_n - W_r) \tag{6}$$

Where:
D = Reaction zone depth (front to rear). ft.
W_n = Net initial fuel loading. lb./ft. ^{2}
W_r = Residue loading immediately after passage of the reaction zone. lb./ft.^{2}

Equation 6 does not account for minerals or water content so the formula was later adjusted to account for that.

4.1.5 Reaction Velocity (Γ)

The next step in creating the model was to find the reaction velocity. The reaction velocity is the ratio of the reaction zone efficiency to the reaction time and can be represented by equation 7.

$$\Gamma \equiv \frac{\eta_\delta}{\tau_R} \tag{7}$$

To fully utilize the reaction velocity, the fuel moisture and the mineral content must be known as that would lead to a slower reaction velocity if there is more moisture within the fuel or more noncombustibles (minerals). By incorporating both the moisture content and the mineral content as a damping coefficient, the equation then becomes:

$$\Gamma = \Gamma^{'} \eta_M \eta_s \tag{8}$$

Where:
$\Gamma^{'}$ = Potential reaction velocity. min $^{-1}$
η_M = Moisture damping coefficient having values ranging from 1 to 0, dimensionless.
η_s = Mineral damping coefficient having values ranging from 1 to 0, dimensionless.

4.1.6 Moisture and Mineral Damping Coefficient

The moisture and mineral damping coefficients as well as the reaction velocity need to be found through experimentation. To find the moisture damping coefficient, three fuel beds of ponderosa pine needles were tested over a wide moisture range. They found the moisture damping coefficient is dependent not only on the moisture but the fuel type as well since logging slash is much more porous and carries more moisture. To obtain the equation for the moisture damping coefficient the authors created a plot (as seen in Figure 1) by comparing the fuel moisture of extinction (where the fire will no longer spread) to the fuel moisture. They then fit the curve and set that as the equation for the moisture damping coefficient.

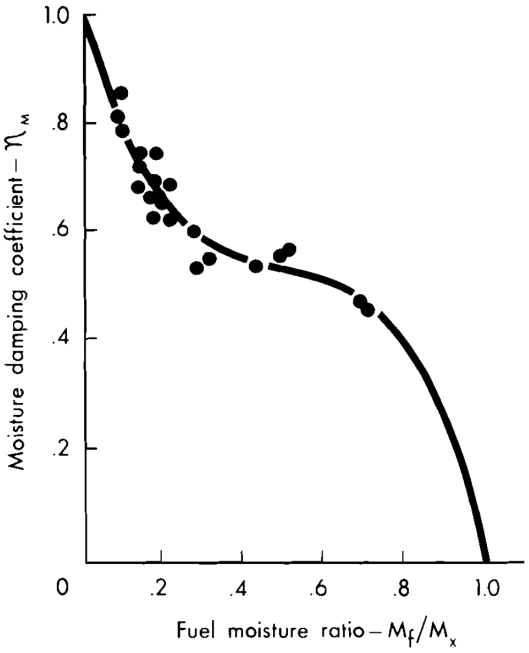

Figure 1: Determining the moisture damping coefficient.

The equation the authors found that fits the curve in Figure 1 is:

$$\eta_M = 1 - 2.59\frac{M_f}{M_x} + 5.11(\frac{M_f}{M_x})^2 - 3.52(\frac{M_f}{M_x})^3 \tag{9}$$

Where:
M_f is the fuel moisture.

M_X is the fuel moisture of extinction.

To find the mineral damping coefficient, the authors assumed the ratio of the "normalized decomposition rate would be the same as the normalized reaction intensity" [Rothermel, 1972]. They then used the maximum decomposition rate and found the mineral content was at 0.0001 which was the lowest fractional mineral content for natural fuels. By then looking into silica-free ash, the authors were able to create another plot as seen in Figure 2. They then found the equation fitting the curve and set that as the mineral damping coefficient. To find the damping coefficient, all the user needs to input is the effective mineral content (silica free).

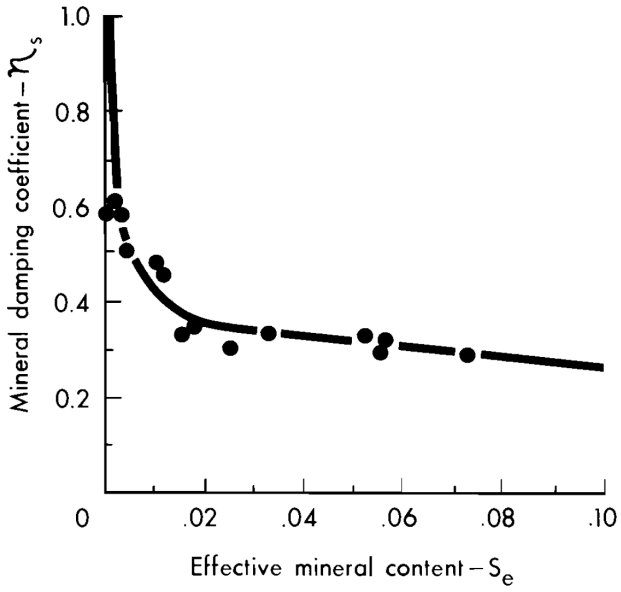

Figure 2: Determining the mineral damping coefficient.

Similar with the moisture damping coefficient, the authors fit this curve and set that as the mineral damping coefficient.

$$\eta_S = 0.174(S_e)^{-0.19} \tag{10}$$

Where:
S_e is the effective mineral content (silica free).

4.1.7 Fuel Packing Ratio (β) and Surface Area to Volume Ratio (σ)

The last parameters are the fuel packing ratio and the surface area to volume ratio. Both of these are fuel properties that to be specified within the fuel parameter for the model to work. These parameters are necessary as they determine how intense a fire may be. With a high packing ratio, there will be a low air-to-fuel ratio and this will make it difficult for the flame to penetrate to the top of the fuel. A more sparse fuel bed will result in a low intensity fire as there will be significant heat losses between the fuel and flame. Finding the optimal packing ratio to achieve the maximum fire intensity is a challenging task as it is likely different for each fuel. The packing ratio can be defined by equation 11.

$$\beta = \frac{\rho_b}{\rho_p} \tag{11}$$

Where:
β = Packing ratio, dimensionless.
ρ_b = Fuel array bulk density, lb./ft^3
ρ_p = Fuel particle density, lb./ft^3

The surface area to volume ratio (SAVR) for fuels is used to quantify the fuel particle size can be represented by equation 12

$$\sigma = \frac{4}{d} \tag{12}$$

Where
d = The diameter of the circular particles or edge length of square particles, ft.

4.1.8 Fitting Missing/Unknown Parameters Through Experimentation

With the whole model setup, the next task was to find the parameters that could only be found through experimentation. This includes the parameters in the reaction velocity, and the slope and wind coefficients. To find the reaction velocity parameters, multiple fuel beds were setup on weighing platforms so the weight of the fuel could be constantly measured. This allowed them to determine how fast the fuel was burning since they had multiple weight sensors at each part of the fuel. With this knowledge, they found that the mass loss rate related to the net initial fuel loading, reside loading, and the width of the weighing platform. Combining this with equation 7 yields equation 13.

$$\Gamma = \frac{\dot{m}}{w_n R W \tau_R} \tag{13}$$

Where:
$\dot{m}$ = Mass loss rate obtained from the weight loss data.

With this final equation, it can then be combined with equation 8 to get the potential reaction velocity and have it now correlated with the physical features of fuel.

$$\Gamma^{'} = \frac{\Gamma}{\eta_M \eta_S} \tag{14}$$

With all the initial equations formulated, experiments were conducted using this model and comparing it to the observed ROS. The first parameter tested within the model to observations is the reaction velocity. In particular, they wanted to find the optimum packing ratio and the optimum reaction velocity. After numerous experiments, they found there is an optimum fuel load for each fuel size. To incorporate this into the model, they combined the maximum reaction velocity with the regular reaction velocity equation and an arbitrary variable A was inserted to better fit the observation. The final equation for the reaction velocity then became:

$$\Gamma^{'} = \Gamma^{'}_{max}(\frac{\beta}{\beta_{op}})^A \exp[A(1 - \frac{\beta}{\beta_{op}})] \tag{15}$$

Where:
A = $\frac{1}{(4.77\sigma^{.1} - 7.27)}$

These equations were designed to fit not only the dependent variables but also the data obtained in their experimentation. These equations are specifically made for reasonable output values even when the input values may be extreme so the model should never result in a negative value.

Next is the propagating flux. To first evaluate the equations, the authors assumed no wind and no slope to make formulating these equations much more simple. The initial equation for the propagating flux can be seen in equation 16.

$$(I_P)_o = R_0 \rho_b \epsilon Q_{ig} \tag{16}$$

To relate the propagating flux to the reaction intensity, a ratio (ζ) was computed and can be seen in equation 17.

$$\zeta \equiv \frac{(I_p)_o}{I_R} \tag{17}$$

The values for ζ are computed and plotted in Figure 3 as a function of β for three fuel sizes. After finding a correlation for ζ as a function of β and σ, Rothermel found ζ can be represented by equation 18.

$$\zeta = (192 + 0.259\sigma)^{-1} \exp[(0.792 + 0.681\sigma^{0.5})(\beta + 0.1)] \tag{18}$$

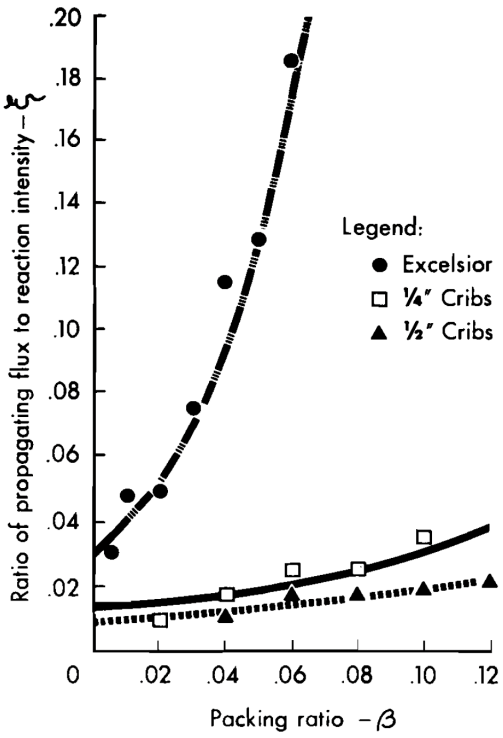

Figure 3: Determining ζ using three different fuel sizes.

4.1.9 Initial ROS Equation

With the missing parameters (with the exception of slope and wind) found, the ROS equation without slope and wind was finished and can be seen in equation 19. This equation meets the initial goals as it is a simple mathematical model that can quickly and accurately calculate the ROS of a fire in no slope and no wind conditions.

$$R = \frac{I_R \zeta}{\rho_b \varepsilon Q_{ig}} \tag{19}$$

4.1.10 Wind and Slope Coefficients

To evaluate the wind and slope coefficients, the authors assumed the fuel type would remain constant. After performing multiple experiments with varying fuel beds at different wind speeds and using field data, they got the wind coefficient to be a function of σ along with the packing ratio and many other constants to match the observed data. The wind coefficient can be seen in equation 20. The slope coefficient was calculated by performing experiments on fuel beds at different slopes. They then found a correlation of the data collected from the experiments and used that as the slope factor and this can be seen in equation 21.

$$\phi_W = CU^B \left(\frac{\beta}{\beta_{op}}\right)^{-E} \tag{20}$$

$$\phi_S = 5.275\beta^{-.3}(\tan\phi)^2 \tag{21}$$

Where:
U = Wind Velocity (ft/min)
C = $7.47\exp(-0.133\sigma^{0.55})$
B = $0.02526\sigma^{0.54}$
E = $0.715\exp(-3.59 * 10^{-4}\sigma)$
ϕ = Slope of the fuel bed.

4.1.11 Final Rate of Spread Equation

The final ROS equation was finally complete and it now incorporates both slope and wind components and is able to be used operationally. There is no longer any calculus needed or any complex calculations. The final equation can be seen in equation 22.

$$R = \frac{I_R \zeta (1 + \phi_W + \phi_S)}{\rho_b \epsilon Q_{ig}} \tag{22}$$

4.2 Balbi Model

2007 Balbi Model

With multiple versions of the Balbi model, the very first model will be discussed followed by the newest version to see how much the model has changed since the original model. The Balbi model is a fully physical model so there will be no observations used in this paper, only physical properties of fires.

4.2.1 Simplified Flow and Flame Tilt Angle

The first parameter in the Balbi model is the simplified flow and the flame tilt angle. These parameters are first calculated assuming no slope and no wind conditions (like with the Rothermel model initially). They assume the main effect of the flow that must be accounted for is the tilting of the flames under wind and/or slope conditions [Balbi et al., 2007]. For the initial study they assumes that under no wind and no slope conditions the flame tilt angle γ equals β_w which results from the buoyancy and the wind. β_w is given by:

$$\tan \beta_w = \frac{\nu_w}{u_{fl}} \tag{23}$$

Where:
ν_w and u_{fl} represent the free stream wind speed and the upward gas flow velocity in still air at mid flame height.

With the introduction of a slope, γ changes as the gas velocity changes due to indrafts (ν_s) and the slope angle (α_0). The relationship can be seen in equation 24 and equation 25.

$$\gamma = \alpha + \beta_s \tag{24}$$

$$\tan \beta_s = \frac{\nu_s}{u_{fl}} \tag{25}$$

For circumstances where there are both wind and slope conditions, they assume the gas velocity induced from the slope factor is negligible in regards to the wind speed.

4.2.2 Simplified Flame Sub-Model

Flame height

To be able to calculate ν_w and u_{fl} and keep the model computationally fast, many simplifying assumptions are made to generate a simple model. The authors split the flame into two different categories, the flame base and the flame body. The flame base will be attached to the fuel bed, and D will be the depth of the fuel bed and h is the height. The flame body is the fire plume and l will represent the depth and H is the flame body height. They then split the calculation up into 6 sections: Flame height, State Equation, Vertical Momentum Equation, Mass Balance, Stoichiometric Ratio, and Thermal Balance to make formulating the model easier. The first calculation is the flame height. To calculate the flame height, the authors used a previous relationship by Sun et al. (2003) for vegetation fires:

$$H = H^* Q^{\frac{2}{5}} = H^* (\Delta h_{fu} \sigma_{fu} c)^{\frac{2}{5}} \tag{26}$$

Where:
H is the flame height.
Q is the rate of heat release per unit length of fire front.
H^* is a parameter to fit.

Δh_{fu} is the heat of combustion of the vegetative fuel.
σ_{fu} is the surface mass.
c is the rate of fire spread.
To better visualize this, refer to Figure 4.

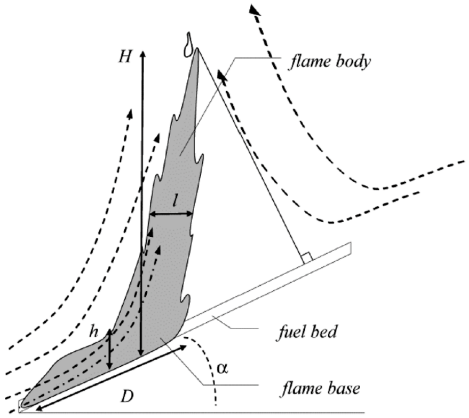

Figure 4: Diagram of the different characteristics of the flame in the 2007 Balbi Paper.

State Equation

For the state equation, the authors "consider the gas state equation for the quasi-isobaric diffusion flame" [Balbi et al., 2007]. This equation can be seen in equation 27.

$$\rho_g T_g = \rho_a T_a \tag{27}$$

Vertical Momentum Equation

As seen in Figure 4, there is a vertical component to the flame. To calculate this component, they first neglect the shear stresses in the gas and instead use buoyancy as the main mechanism involved in the vertical momentum. this is given by:

$$\rho_g \frac{\partial u}{\partial t} = (\rho_a - \rho_g)g \tag{28}$$

To solve for this equation, simple integration along the flame length results in the gas velocity at mid flame, u_{fl}

$$u_{fl} = Q^{\frac{1}{5}} \sqrt{(\frac{T_{fl}}{T_a} - 1)gH^*} \tag{29}$$

Mass Balance

Mass balance is kept simple for the whole flame structure based on the geometry of the flame. In slope and wind conditions, the rate of air entrainment is considered negligible in mass balance. With this assumption, the continuity equation per unit length of the fire can be used and is given by:

$$\rho_g u_{fl} l = \rho_{ga} h \nu_u + D\dot{\sigma}_{fu} \tag{30}$$

Where the left hand side of the equation is the rate of mass loss from the flame body, $\rho_{ga} h \nu_u$ is the rate of air entrainment upward in the flame, and $D\dot{\sigma}_{fu}$ is the rate of mass increase due to the thermal degradation of the vegetation.

Stoichiometric Ratio

The stoichiometric ratio involves the rate of air entrainment upward in the flame and how that is proportional to the rate of mass incoming from thermal degradation, υ being the stoichiometric ratio [Balbi et al., 2007].

$$\rho_a h \nu_u = \upsilon D \dot{\sigma}_{fu} \tag{31}$$

Thermal Balance

The last parameter in the flame sub model is the thermal balance. The thermal balance calculates the temperature of the flame and has the same assumptions as the continuity equations. After simplifications and rearranging the initial equation, as well as assuming the specific heat is held constant in the flame, fuel gases, and that the fuel gases are emitted near the ambient temperature, the equation for the flame temperature becomes:

$$T_{fl} = T_a + \frac{(1-\chi)Q}{(\upsilon+1)D\dot{\sigma}_{fu}c_{pg}} = T_a + \frac{1-\chi)\Delta h_{fu}}{(\upsilon+1)c_{pg}} \tag{32}$$

4.2.3 Simplified radiation Sub-Model

When a fire front spreads, there is a radiant heat flux impinging on the unburnt fuels ahead of the flame front [Balbi et al., 2007]. This component is split up into two different components. The radiative component from the flame base, and the flame body radiation. For the flame base radiation, they assume the emissivity of the flame base is equal to unity [Balbi et al., 2007], which results in:

$$R_b = \sigma T_{fl}^4 \mathrm{d}(\delta - x) \tag{33}$$

Where: T_{fl} is the flame temperature (calculated in equation 32) $\delta = 4/\alpha_{fu}\zeta_{fu}$ is the mean penetration distance of radiation within the fuel bed. "x is the coordinate in space normal to the fire front and d represents the fuel depth" [Balbi et al., 2007].

When flames are on a slope or under windy conditions, the flame is brought closer to the unburnt fuel, which preheats the fuels more than if the flame were vertical. The base radiation would stay the same under any conditions. The amount of radiation is a complex calculation however since the amount of radiation reaching the unburnt fuel from the flame body must be integrated the length of the flame as well as using an inverse square law to find the distance r between the two areas [Balbi et al., 2007]. To reduce this equation to be used in a simplified model that is faster than real time, an assumption that the fire front is a flame panel with height H and infinite width from a surface fuel element (Balbi, 2007). The equation then becomes:

$$R_{fl} = \epsilon_{fl}\sigma\frac{T_{fl}^4}{2}(1-\cos\theta) \tag{34}$$

Where:
θ is the angle between the base of the flame panel and the element of surface fuel.

4.2.4 Preheating Sub-Model

This is the last submodel in the 2007 Balbi model. In this submodel, the authors introduce the relationship for the ROS under low Speed Regimes, relationship for the ROS under high speed regimes, and a simplified model of fire spread under high speed regimes. The major assumption here is the radiation is denoted as the prevailing form of heat transfer in fire spread. Like with the Rothermel model, calculations are first made with no wind no slope conditions to simplify calculations and those parameters are added in later. With no wind no slope conditions, the fire propagation will remain relatively constant for a given fuel. Whereas with wind or a slope, that will introduce a flame tilt and thus preheat the fuels ahead of the fire much more effectively. The base equation for the preheating sub model (which also represents the thermal balance for the unburned fuel ahead of the fire front) is as follows:

$$\sigma_{fu}c_{pfu}\frac{\mathrm{d}T_{fu}}{\mathrm{d}t} = R_b + R_{fl} - \Delta h_w \frac{\mathrm{d}\sigma_w}{\mathrm{d}t} \tag{35}$$

Under a low speed regime, γ will likely remain close to 90° as there is no slope or little to no wind pushing the flame closer to the unburnt fuel. As a result, R_{fl} can be neglected in this case and equation 35 can be

solved with neglecting the flame body radiation. After substitutions and some manipulation of equation 35, the resulting equation is:

$$c_1 = \frac{\sigma T_{fl}^4 \mathrm{d}\delta^2}{2\sigma_{fu}(c_{pfu}(T_{ig} - T_a) + \Delta h_w \eta)} \tag{36}$$

Where:
c_1 = constant ROS. dx = $c_1 \mathrm{d}t$ η = moisture content defined by $\eta = \sigma_w / \sigma_{fu}$

On the other hand, with a high speed regime, the flame body radiation is assumed to be the main form of heat transfer to the unburned fuels. As a result, R_b is negligible and can be omitted in these calculations. By assuming that the ROS is constant over the space interval from 0 to Hsin γ, equation 35 can be integrated and solved as:

$$c_h = c_l + \frac{\epsilon_{fl}\sigma T_{fl}^4 H}{2\sigma_{fu}(c_{pfu}(T_{ig} - T_a) + \Delta h_w \eta)}(1 + \sin\gamma - \cos\gamma) \tag{37}$$

Sine c_l is negligible as the flame body is the main contributor to the ROS, it can be removed from equation 37.

The final parameter is the simplified model of fire spread under high-speed regimes. First the authors define how much heat is actually transferred from the flame to the unburnt fuel. This is given by:

$$\varepsilon_{fl}\sigma T_{fl}^4 = \chi Q / H \tag{38}$$

To further reduce this model to reach the final form, the fraction of radiation χ decreases with flame width according to a parameter q that must be fitted in experimentation later on [Balbi et al., 2007].

By combining all the above equations together, both no slope no wind and conditions with slope and wind, it results in a large series of simplified nonlinear equations. Since there is no longer a need for calculus or solving partial differential equations, this model has succeeded in becoming simple enough for a computer to solve quickly. To test the speed of the model, the authors simulated a fire front shape, and found the ROS at specific points along the fire front. Usually, a grid would be constructed to help in solving this, but the authors utilized Mathematica to represent the fire front shape on a three dimensional domain. By using this technique, they found the computational time is lower than real time [Balbi et al., 2007]. Now all that is left for the model is validating it using lab and experimental burns and fitting parameters. Some of the parameters they found remained relatively constant throughout the different burns (ex: q = 3), but the other parameters varied with different fuels characteristics.

To calculate the wind and slope parameters, the authors initially used multiple high speed regimes to calculate how slope and wind would impact the fire spread (these calculations can be seen in equation 39 and equation 40). They then used multiple laboratory and field experiments in different slopes and wind speeds to observe how the flame behaves in different conditions and verify their calculations. In slopes and windy conditions, the authors realized with a greater slope or greater wind speed, that would change the flame tilt angle and the flame height which would bring the flame closer to the unburnt fuel. After comparing the model to numerous datasets, the authors kept getting different values for the wind and slope coefficients (which they expected). They found these parameters vary with different fuel properties. With a greater fuel height, fuel load, and SAVR, then there would be more fuel to burn and the flame body radiation can reach the fuel much more effectively. With a greater FMC, then the flame would take more energy to dry out the fuel, slowing down the ROS.

$$\begin{cases} \frac{c_h}{c_l} = A(1 + \sin\gamma - \cos\gamma)^q \\ \gamma = \alpha + \beta_s \\ \tan\beta_s = b_s c_h^{3/5} \end{cases} \tag{39}$$

Where:
$b_s = \frac{\tau}{0.08(\Delta h_{fu}\sigma_{fu})^{2/5}}$

$$\begin{cases} \frac{c_h}{c_l} = A(1 + \sin\gamma - \cos\gamma)^q \\ \gamma = \alpha + \beta_w \\ \tan\beta_w = b_w \nu_w c_h^{-1/5} \end{cases} \tag{40}$$

Where:
$b_w = \frac{1}{0.2\sqrt{(\frac{T_{fl}}{T_a} - 1)g(\Delta h_{fu}\sigma_{fu})^{1/5}}}$
A = $(\frac{0.15\Delta h_{fu}}{C_{pfu}(T_{ig} - T_a) + \Delta h_w \eta})$

4.2.5 Wind and Slope

2022 Balbi Model

With many other revisions to this model (such as the 2009 paper and 2020 paper), this model has undergone a lot of change and this will be evident by the amount of change in the 2022 Balbi paper. The most notable difference is a convective component was added to the model. Before, the model only considered the flame base radiation and the flame body radiation, but now there is a convective component that helps spread the fire in a similar location as the base radiation according to Figure 5. This component is based on the inflow of hot gases from the lower part of the flame base.

Figure 5 is essentially what the 2022 model follows. There is the flame body radiation, flame base

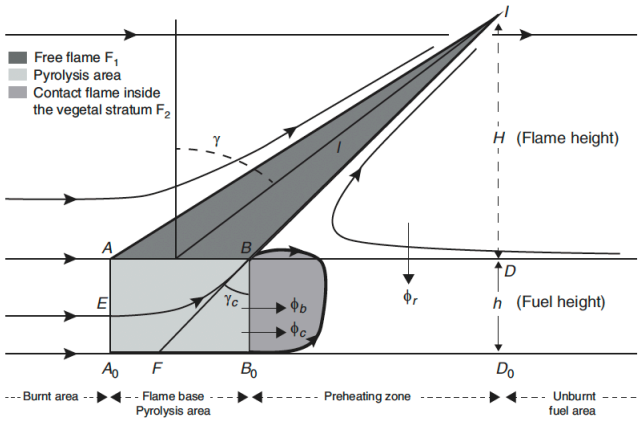

Figure 5: Diagram showing the idealized scenario of the flaming zone.

radiation, and the convective radiation. The convective component was originally introduced in the 2020 Balbi paper. That paper was created in a laboratory setting and was advertised as able to be used in a field setting. After extensive testing, the developers created another model (the 2022 model) and changed some parameters (as well as introduced more).

Since the other two parameters (R_b and R_{fl}) have been discussed, those will not be discussed again. Instead, the main focus will be on the convective component as that has proven to be one of the most sensitive parameters within the model. The convective component is initially modeled as:

$$\phi_c = \frac{\Delta H}{2\tau_0}\sigma s min(h, \delta)\tan\gamma_c \tag{41}$$

Where:
ΔH and τ_0 are the heat of combustion of pyrolysis gases and the flame residence time parameter [Chatelon et al., 2022].

The angle γ_c is defined as :

$$\tan\gamma_c = \tan\alpha + \frac{U(L)}{u_c} \tag{42}$$

. Where U(L), u_c, and α are horizontal wind speeds at point B [Chatelon et al., 2022]. U(L) is further expressed as a function of the wind velocity at mid flame and accounts for drag forces. After some simplifications and substitutions, the authors found the final equation for the convective component R_c:

$$R_c = a_M min(\frac{W_0}{50}, 1)\frac{\Delta H \rho_a T_a s\sqrt{h}}{2q(s_t+1)\rho_v T}(\frac{(s_t+1)\rho_v T}{\tau_0 \rho_a T_a} min(S, \frac{2\pi S}{S_t}\tan\alpha + U\exp(-\frac{\beta_t}{min(\frac{W_0}{50}, 1)}R)) \tag{43}$$

Where:
R_c = Contribution of convection to the ROS (m/s).
a_M = Fitted model parameter.
W_0 = Ignition line width (m).
ΔH = Heat of combustion of the pyrolysis gases (J/kg).
ρ_a = Air Density (kg/m^3)

T_a = Air Temperature (K)
h = Fuel bed depth (m)
q = Ignition Energy (J/kg)
s_t = Air pyrolysis gases mass ratio in the flame body.
ρ_v = Fuel Density (kg/m^3)
T = Mean flame temperature (K)
τ_0 = Flame residence time parameter (s/m)
S = Leaf area by square meter (m^2/m^2)
α = Terrain slope angle (degrees)
U = Sum of normal component (to the fire front) of the natural wind velocity and fire generated inflow coming from the burnt area (m/s).
β_t = Total packing ratio.
R = Rate of Spread (m/s).

Final Rate of Spread Equation

The final ROS equation is computed by adding up all the components in the fire (the flame base, base radiation, and convective component) and this can be found in equation 44.

$$R = R_c + R_b + R_f \tag{44}$$

Where:
R = Rate of Spread (m/s)
R_c = Convective radiative heat transfer.
R_b = Base radiative heat transfer.
R_f = Flame body radiation.

4.3 Comparison of the Two Models

To test these two models, the models were placed under the same fuel categories (tall grass) and the same environmental conditions. To maximize testing, both models underwent conditions where there was wind and slope present. The base testing occurred in 1.5m/s winds and a slope of 3 degrees.

The Balbi code used in this experiment was originally developed using the 2018 paper, but has since been updated to the 2020 paper with the help of John Stuart and Dr. Adam Kochanski. This code was made to fit the same values as the developers of the Balbi model using the Kolgerberg experimental dataset from the Van Wilgen experiment. Some assumptions in these experiments are the air temperature will remain constant and the ignition line width will remain constant at 50m (this was later removed in the 2022 paper). Another assumption made for testing the Balbi model in this experiment is the dead fuel load and the total fuel load are the same. With these conditions, the models can be properly tested. All plots will plot the same variables despite changes or not in them. The reason for this is so any change in the rate of spread can be easily identified (such as if the base radiation is the main contributor to the ROS or the wind coefficient).

4.3.1 Wind Speed

In Figure 6, the ROS calculations in the Rothermel model approaches 5m/s. Under extreme conditions such as this, the model handled it well with a realistic approximation for the ROS. The main contributor to the ROS is the wind coefficient which follows the trend of the ROS almost exactly. The other parameters used to calculate the ROS do not change as those plots are blank. The Balbi model on the other hand follows a similar story to the Rothermel model, however the ROS value is much lower as it approaches 3m/s instead of 5m/s. This indicates the Rothermel model tends to over-predict the ROS (assuming the Balbi model is correct) in extreme conditions. Looking at the Balbi model, the main component driving the ROS in this model is the flame body radiation which follows the trend of the ROS. This is due to the flame body being pushed closer to the unburnt fuel, lowering the flame tilt angle (γ) and more effectively preheating the fuel.

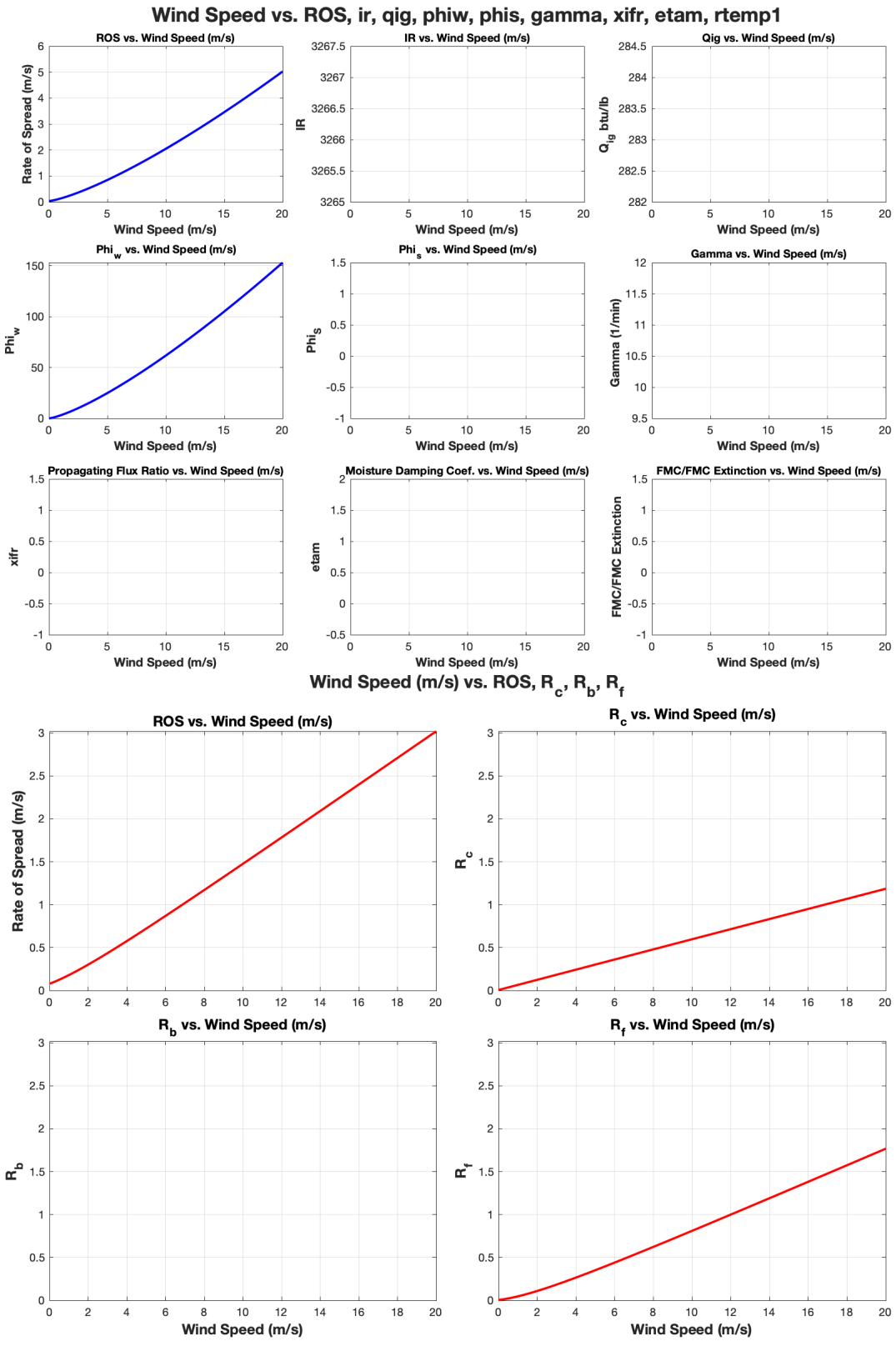

Figure 6: Comparison of the Balbi model and Rothermel model under wind speeds from 0-20m/s.

4.3.2 Slope

The next component tested is the slope. In Figure 7 the two ROS models follow the same exponential pattern, but the Rothermel model begins to produce unrealistic results as the slope approaches 80 degrees. The slope coefficient is the main contributor for the ROS as the curves are identical. The model remains below 6m/s until about 70 degrees where the ROS values begin to increase exponentially until 40 m/s. An image of this behavior can be better seen in Appendix A in figure 13. On the other hand the Balbi model remains at reasonable values with the ROS around 3m/s with the convective coefficient being the main driver for the ROS. With a greater slope, the flame body radiation also increases like with Figure 6.

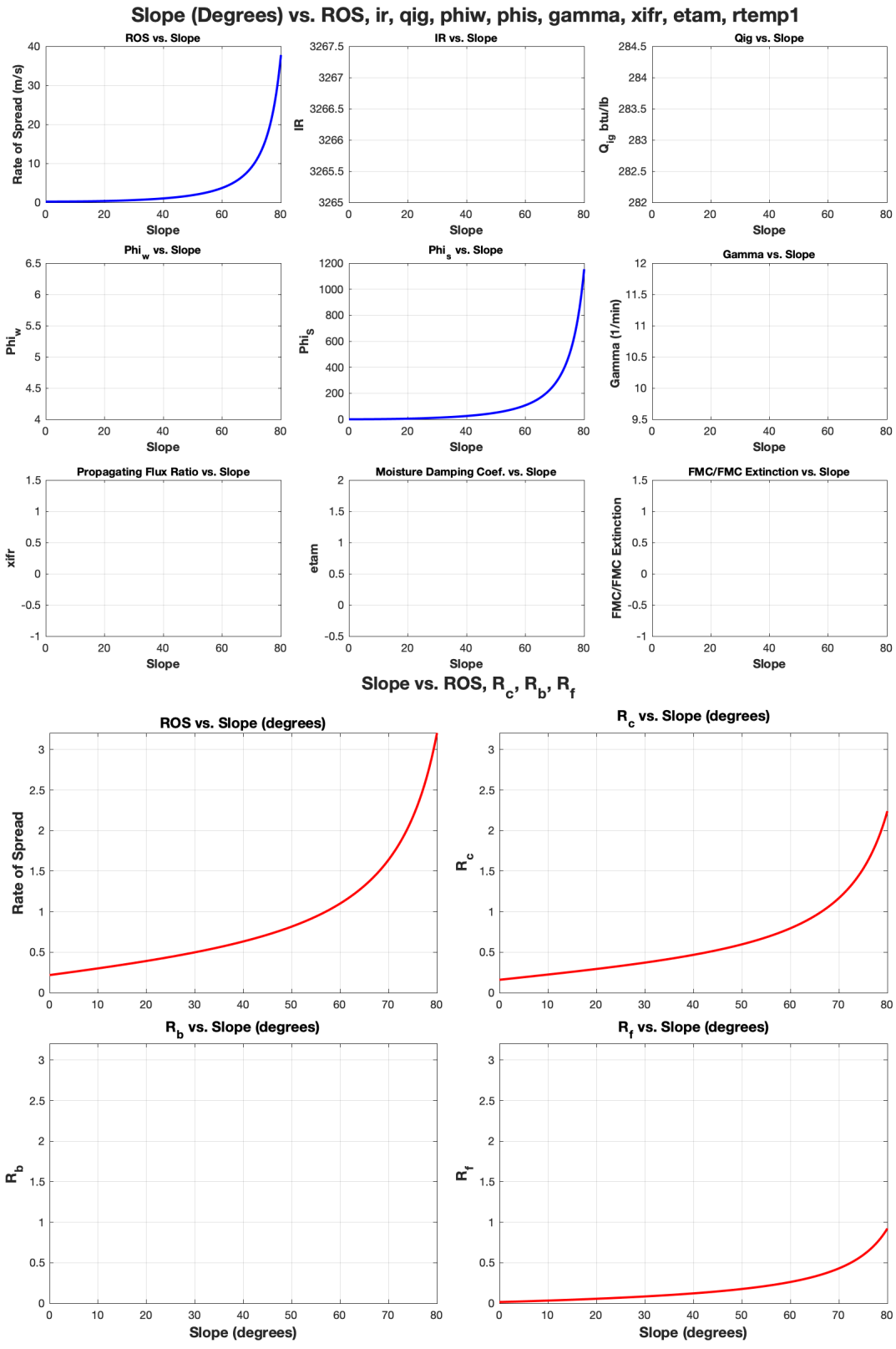

Figure 7: Comparison of the Balbi model and Rothermel model under varying slopes from 0-80 degrees.

4.3.3 Fuel Moisture

FMC with slope and wind

In Figure 8 there is a decrease in the ROS with an increasing fuel moisture. With more moisture in the fuel, that means more energy is required to dry out the fuel so it can burn, which slows down the ROS. Something to note here is that the FMC in the Rothermel model only goes to about 25%. In the model there is the fuel moisture of extinction parameter and that will start causing the model to result in negative values if the fuel moisture is greater than the fuel moisture of extinction. There are many components involved in the fuel moisture calculation in the Rothermel model and their overall influence on the ROS can be seen in Figure 8. The moisture damping coefficient, reaction intensity, and optimum reaction velocity all decrease with an increase in the fuel moisture content. The Balbi models ROS also decreases with an increase in FMC. Since this experiment contained both wind and slope, both R_c and R_f contributed to the overall ROS. Unlike with the previous plots R_b decreased with an increase in FMC. To further evaluate the changes from FMC, further tests were done and can be seen in Figure 9 where the experiment occurred under no slope and no winds conditions, and Figure 10.

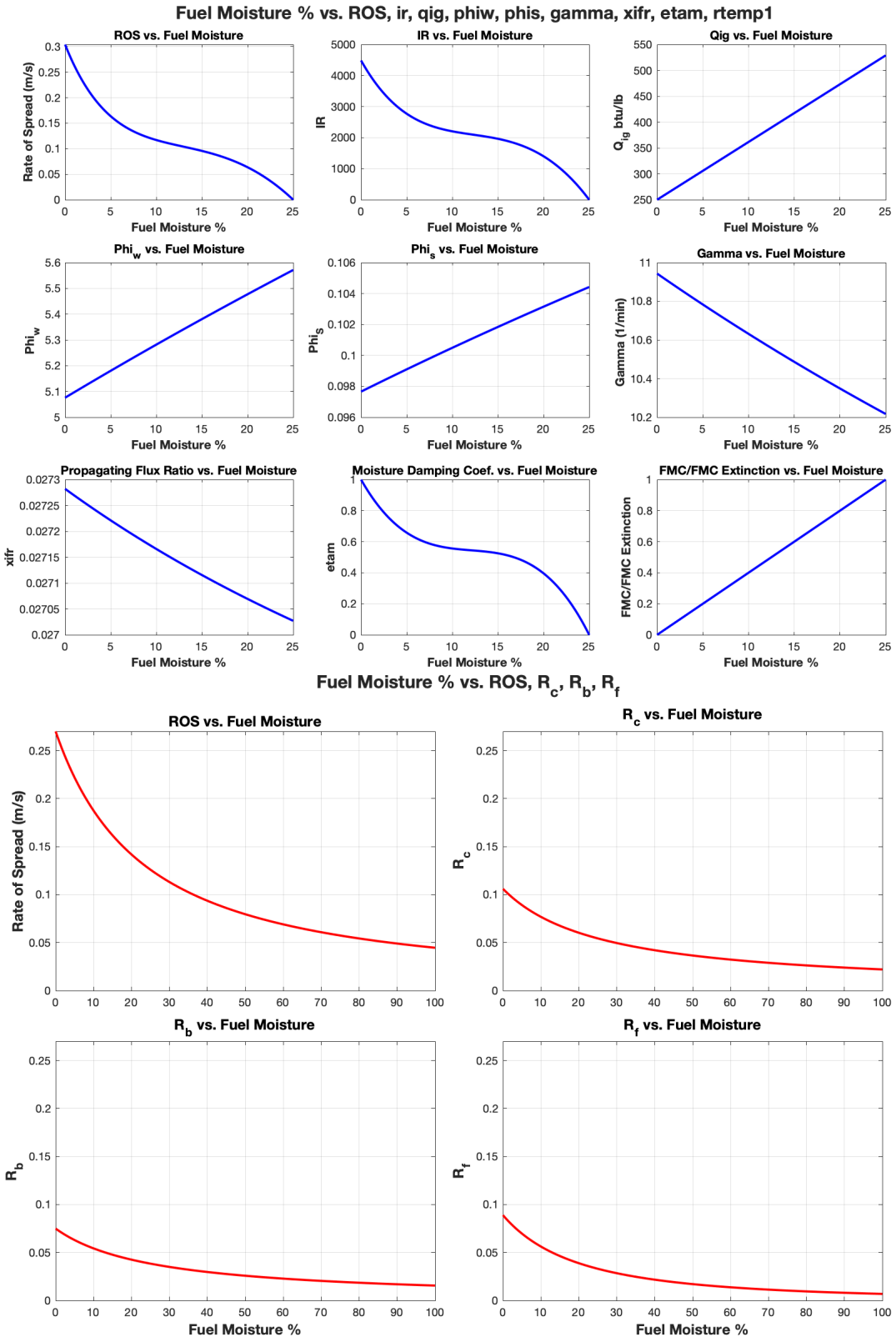

Figure 8: Comparison of the Balbi model and Rothermel model under varying fuel moistures.

Fuel Moisture Without Wind and Slope

Figure 9 plots the FMC under no wind and no slope conditions to see how the ROS changes with just the FMC. Overall the ROS has decreased in both plots which is to be expected since there is no longer any preheating from convection or flame body radiation. Instead the base radiation is the only contributor to the ROS in both models.

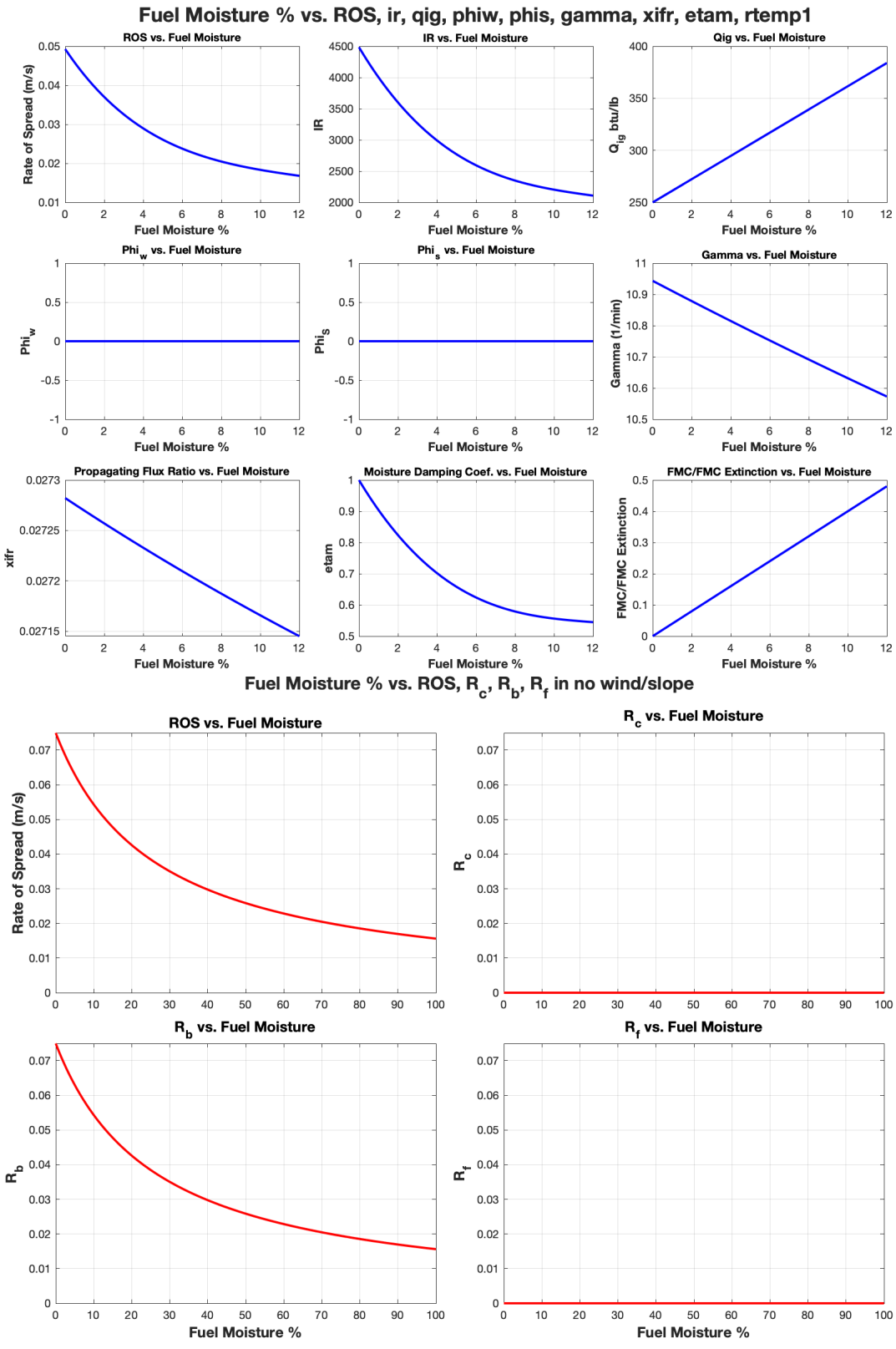

Figure 9: Comparison of the Balbi model and Rothermel model under varying fuel moistures without wind or slope.

Fuel Moisture past Fuel Moisture of Extinction

This part is mostly to see how the Rothermel model reacts to fuel moistures greater than the fuel moisture of extinction. A plot of this can be seen in Figure 10. The ROS decreases exponentially and the main contributor to this decrease is from the moisture damping coefficient. With more moisture, the fire will no longer be able to spread one it reaches the threshold. As it approaches the threshold, the ROS declines. Once it exceeds the threshold, then the ROS becomes negative since there is too much moisture in the fuel for a fire to spread. This parameter is not in the Balbi model since the Balbi model is physics based. The Balbi model would only account for how much heat it takes to preheat these wet fuels and ignite them. This process would greatly reduce the ROS if there is more moisture which can be seen in figure 9.

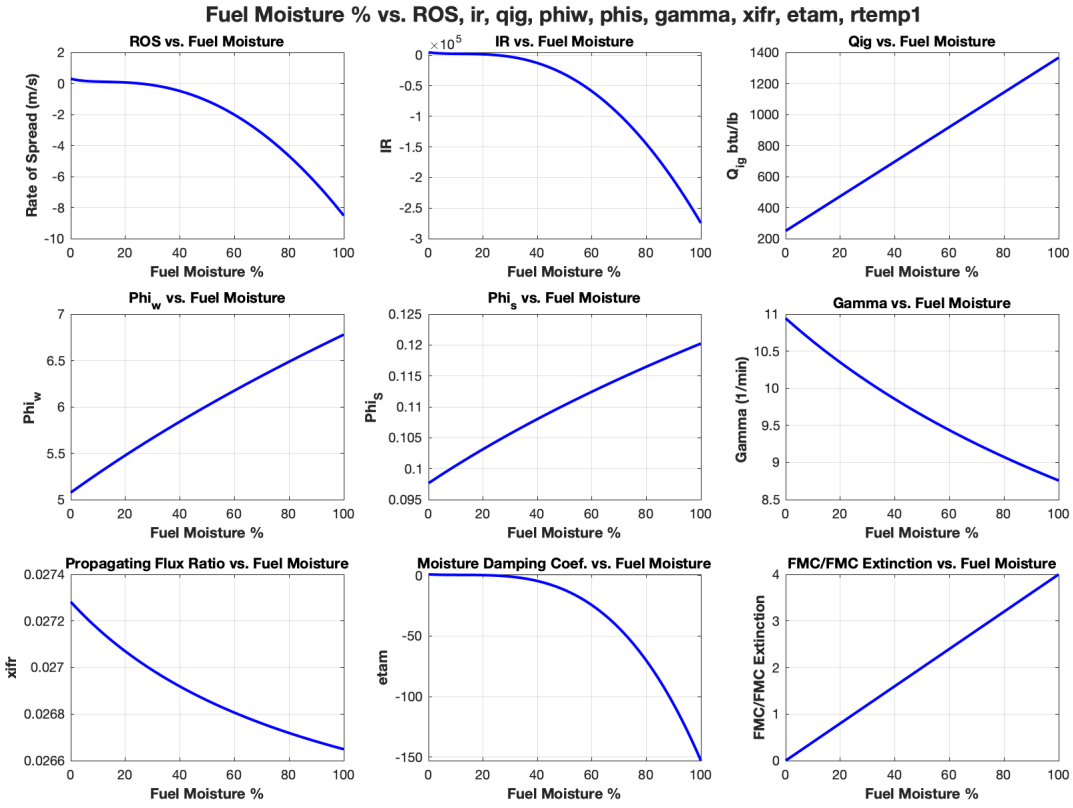

Figure 10: Rothermel Model FMC without fuel moisture of extinction in mind.

4.3.4 Fuel Height

The next parameter tested was the fuel height. To test this, an array of 1000 values ranging from 0-20m were input into the model to see how the ROS changes with varying fuel heights. The results can be seen in Figure 11. The Rothermel model quickly increases with an increase in the fuel height. The main contributor to the increase are the slope and wind parameters. With an increase in fuel height, there is more area for the flame to preheat, making it easier for the fire to spread. Since the experiment occurred on a slight slope and a small wind, these effects amplify when there is more area for the fuel to preheat. In terms of the Balbi model, interestingly the flame body radiation does not contribute much to the ROS. Instead the convective component and the base radiation are the main contributors to the ROS. Looking further into the Balbi model, the fuel depth is used in every parameter in the final ROS equation. With a greater fuel depth, the packing ratios decreases, and the amount of drag increases. As the packing ratio decreases, there is not as much fuel to preheat so the flame body can not preheat as much fuel, thus, not contributing as much to the overall ROS.

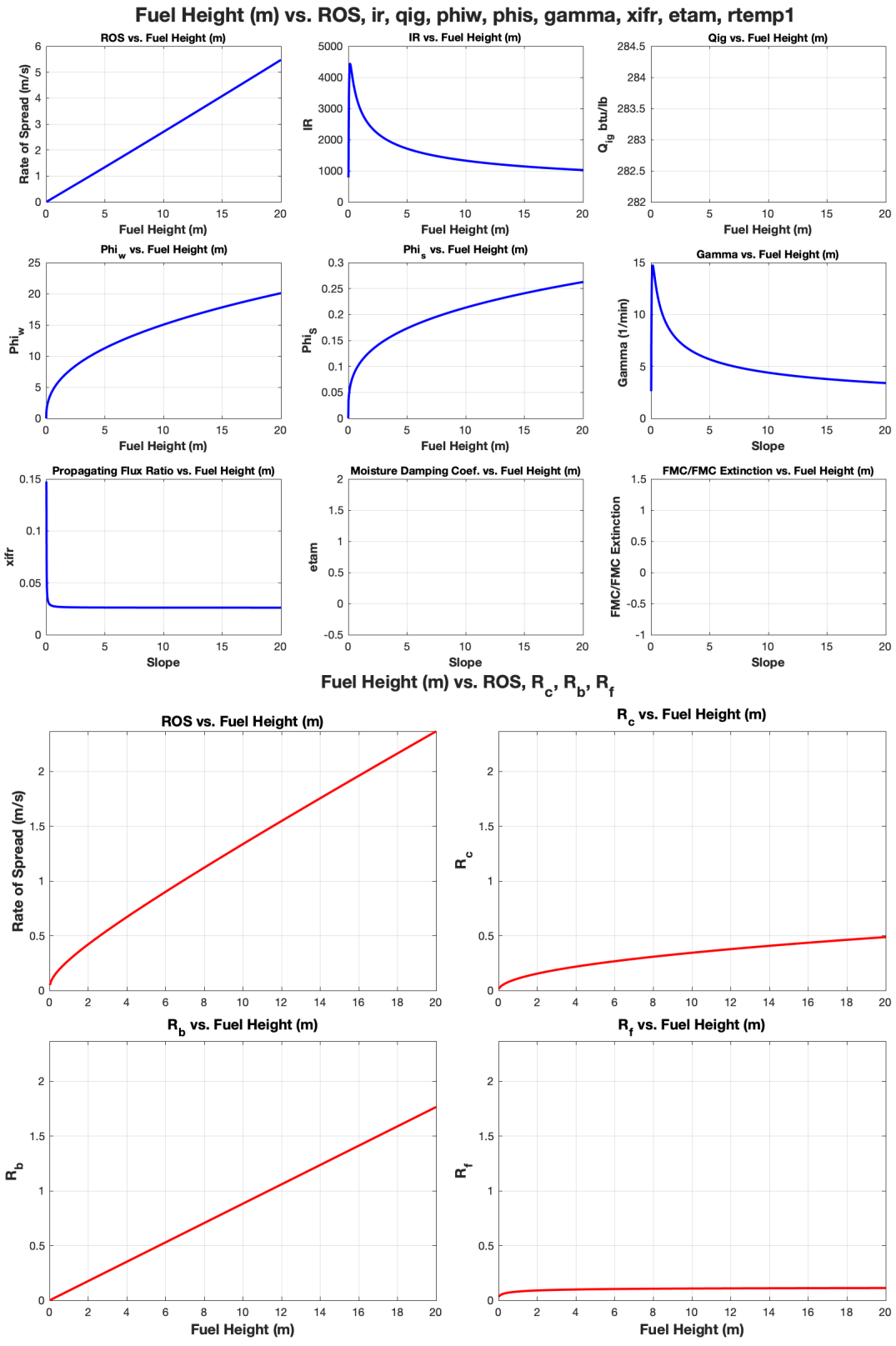

Figure 11: Comparison of the Balbi model and Rothermel model under varying fuel heights.

4.3.5 SAVR Comparison

With an increase in the SAVR, both models exhibit different behaviors. In Figure 12, the Rothermel model quickly increases then decreases. As the SAVR increases, wind coefficient contributes less, whereas the optimum packing ratio and the reaction intensity both increase with an increase SAVR indicating the wind coefficient is the main contributor until a certain point then the other components begin to take over. In terms of the Balbi model, the convective component is the main contributor to the ROS with a little help from the flame body and base radiation int eh beginning, but they quickly flatten out.

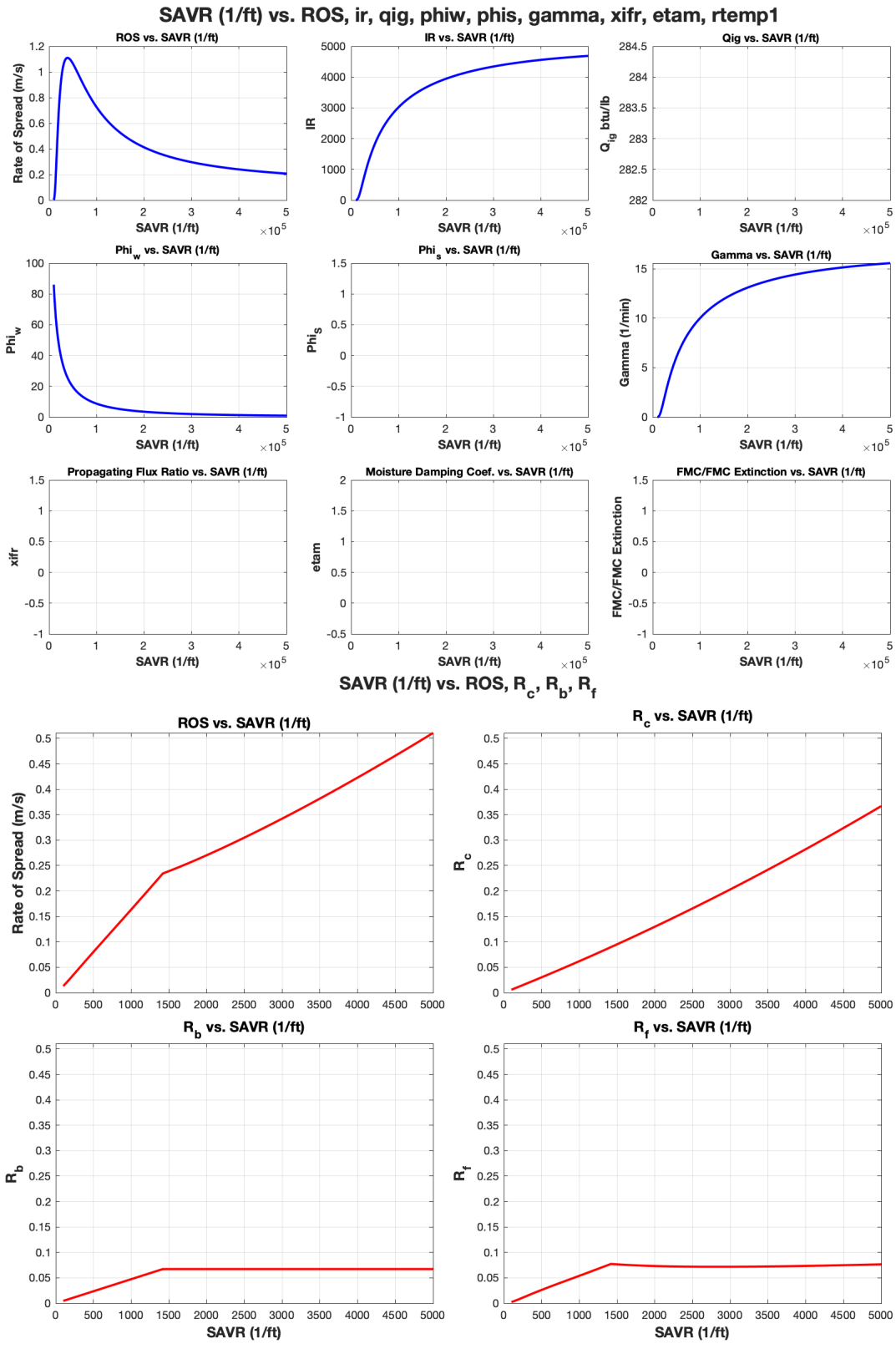

Figure 12: Comparison of the Balbi model and Rothermel model under varying fuel SAVR's.

5 Discussion

Both the Balbi model and Rothermel model have proven to be useful and reliable in certain environments despite the differences between them. By using observational and statistical data, and physical properties, the Rothermel model is relatively limited on the conditions it can be used in. With FMC values greater than that of the fuel moisture of extinction, the ROS will quickly become negative which would likely cause issues in larger models. The Balbi model only relying on physical properties puts it at an advantage since it can account for more extreme weather and fuel conditions and not have issues converging to a realistic solution. Both models had similar assumptions in the beginning by assuming no slope no wind conditions, but they quickly diverged from each other. The Rothermel model was developed based on the heat balance model in equation 1 and made several assumptions based on observations and physical properties. The Balbi model uses equations based on various heat transfers and forms equations based on that concept instead of relying on just one principle and simplifying that down. The Rothermel model also considers different properties of heat transfer than the Balbi model. In the Rothermel model, processes such as the reaction intensity, heat of preignition, and reaction velocity are used to calculate the ROS. In the Balbi model, the authors utilize similar concepts such as the preheating sub model, but it mostly relies on how much heat is transferred to unburnt fuels and what processes are causing that to occur (such as the base radiative component and flame body radiation).

In terms of the wind and slope coefficients, these were approached similarly in the models by using experimental data to better fit the parameters. These parameters were then related to fuel and weather conditions as they vary under different conditions. The overall equations for them varies since the models were built with different approaches. With no flame body radiation in the Rothermel model, the slope and wind parameters become the main contributors to the ROS which can be seen in the above graphs with wind and slope varying. Whereas with the Balbi model, most parameters change with the exception of the base radiation. With a greater wind and slope, there are more in drafts into the fire, increasing the convective and flame body heat transfer.

6 Conclusion

Both of the models excel at their main goal which was to provide an accurate ROS model that can be computed quickly and provide a mostly accurate result. With all the simplifications and assumptions made to create these models, they perform well enough to warrant using them for real world applications. When it comes to extreme conditions, the Balbi model performed much better than the Rothermel model. With extreme wind speeds and extreme slope angles the Rothermel model resulted in ROS above 10m/s whereas the Balbi model provided a much more reasonable ROS. The Rothermel model also struggled with FMC values as the ROS quickly became negative when the FMC approached and exceeded the fuel moisture of extinction. This was not the case in the Balbi model as the Balbi model accounts for high FMC in the fuel and calculates how much heat it would take to dry out the fuel and ignite it. That is where some of the main differences between these models come in. By using purely physical properties to create a model rather than using physics and observations, the physical model will likely yield a much closer approximation to the ROS since finer scale details are being accounted for and implemented into the model. The Balbi model is constantly being improved as well with another version soon to come that will remove the iterative process from the current model. The Rothermel model has had a few updates throughout the years, but not nearly as many. Running some small base tests on the model this is easily seen as the model seems to over predict the ROS (at least in this dataset it exceeded the observed ROS and the Balbi model). The Rothermel model is still a useful model that can be and is currently implemented into larger models (WRF-SFIRE), but in the future the Balbi model will prove to provide a much more accurate result. With the initial goal of comparing the two models on both an analytical and conceptual basis, these models successfully calculate the ROS using very different approaches and assumptions.

References

Anderson, W. R., Catchpole, E. A. and Butler, B. W. [2010], 'Convective heat transfer in fire spread through fine fuel beds', *International Journal of Wildland Fire* **19**, 284–298.

Balbi, J. H., Chatelon, F. J., Morvan, D., Rossi, J. L., Marcelli, T. and Morandini, F. [2020], 'A convective-radiative propagation model for wildland fires', *International Journal of Wildland Fire* **29**.

Balbi, J. H., Rossi, J. L., Marcelli, T. and Santoni, P. A. [2007], 'A 3d physical real-time model of surface fires across fuel beds', *Combustion Science and Technology* **179**, 2511–2537.

Chatelon, F. J., Balbi, J. H., Cruz, M. G., Morvan, D., Rossi, J. L., Awad, C., Frangieh, N., Fayad, J. and Marcelli, T. [2022], 'Extension of the balbi fire spread model to include the field scale conditions of shrubland fires', *International Journal of Wildland Fire* **31**, 176–192.

Rothermel, R. C. [1972], *A mathematical model for predicting fire spread in wildland fuels*, Intermountain Forest and Range Experiment Station, Forest Service, United States Department of Agriculture.

7 Appendix A

Here is a link to the codes used for this experiment.
Fuels code: `https://github.com/Jeremy-Benik/164/blob/main/Assignments/draft/fuels_mod.m`

Rothermel Code: `https://github.com/Jeremy-Benik/164/blob/main/Assignments/draft/ros_rothermel.m`

Balbi Code: `https://github.com/Jeremy-Benik/164/blob/main/Assignments/draft/ros_balbi.m`

Testing the Balbi Model: `https://github.com/Jeremy-Benik/164/blob/main/Assignments/draft/Testing_Balbi.m`

Testing the Rothermel Model: `https://github.com/Jeremy-Benik/164/blob/main/Assignments/draft/Testing_Rothermel.m`

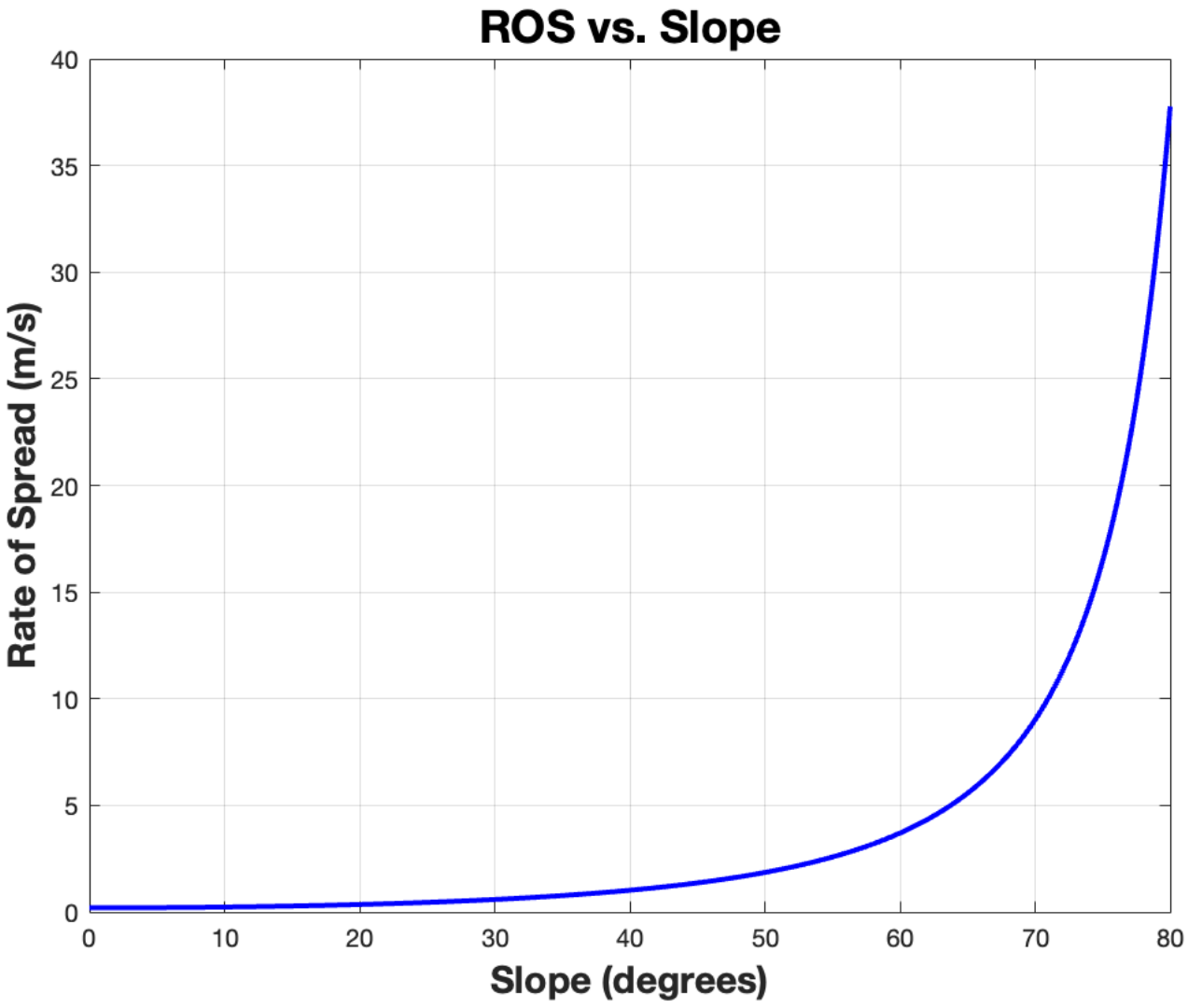

Figure 13: Zoomed in image of slope vs. ROS. The ROS remains relatively stable until 65 degrees where the ROS begins to increase exponentially into unreasonable ROS values.